33rd Annual International Conference of the IEEE EMBS
Boston, Massachusetts USA, August 30 - September 3, 2011

In-vivo MRI and in-vivo electro-anatomical voltage map characteristics of infarct heterogeneity in a swine model

E. Shokrollahi, M. Pop, M. Safri, Y. Yang, P. E. Radau, J. Barry, J. Detsky, G. H. Griffin, E. Crystal, G. A. Wright

Sunnybrook Research Institute, University of Toronto, Toronto, Canada

Abstract— **The arrhythmogenic substrate in patients with prior myocardial infarct (MI) is located at the border zone, BZ. In this study we correlated the BZ identified by two methods: electro-anatomical voltage mapping (EAVM) and a novel MRI method, multi-contrast late enhancement (MCLE). A pre-clinical porcine model with chronic MI was used to characterize BZ via MRI and EAVM. Results focus on the comparison between scar percentage and BZ percentage identified by each method. The correlation coefficient for BZ percentage between the two methods was 0.74 with a p-value of less the 0.0001. Bland-Altman plots were also used to compare between the two methods (slope of 0.83 ± 0.045). For a case of subtle infarct, there was only 1.3% infarct identified on EAVM compared to 22.2% on the corresponding slice on MCLE. The percentage of infarct on MCLE in subtle infarct does not relate to percentage of infarct in EAVM. Future registration between T_1 maps and EAVM will permit a quantitative comparison of MRI and EAVM measures.**

I. Introduction

Assessing the heterogeneity of injured myocardial tissue (e.g. chronic scar) is important for diagnosis and treatment, and depends on accurate electrical mapping and morphological characterization of the arrhythmogenic substrate [1]. During an invasive electrophysiology (EP) study, the scar and the substrate are identified in the electro-anatomical voltage maps, EAVM (e.g. from CARTO Biosense Webster Inc., Diamond Bar, CA) [2]. The substrate is located in the border zone (BZ) areas, at the periphery or traversing the dense scars. BZ has altered action potentials and conduction velocities because of the mixture of healthy and dead myocites (which are electrically inactive). Heterogeneous infarcts can create "reentry circuits" that generate abnormal heart rhythms [3]. Clinically, this heterogeneity is assessed by delayed-enhanced magnetic resonance imaging (DE-MRI) methods, and was found to be independently associated with a higher risk of mortality [4].

Recent studies have tried to correlate EP maps with BZ and scar identified using conventional DE-MRI with Gadolinium contrast agents [5]. A superior MR method that characterizes the infarct heterogeneities was recently applied to a small cohort of patients, and is based on multi contrast late enhancement (MCLE), which provides excellent identification of subtle lesions [6]. However, its correlation with EAVMs has not been investigated. Thus, the specific aim of this study was to compare the MCLE and EAVM methods with respect to the identification of dense scar and BZ, in a swine model of chronic infarction.

Manuscript received April 08, 2011. E. Shokrollahi is with University of Toronto and Sunnybrook Research Institute, 2075 Bayview Ave..Toronto, ON. Canada, M4N 3M5. E. Shokrollahi phone: +1647-822-6163; e-mail: elnaz.shokrollahi@utoronto.ca. M. Pop, Sunnybrook Research Institute, mpop@sri.utoronto.ca. M. Safri, Sunnybrook Research Institute, murtazasafri@gmail.com. Y. Yang, Sunnybrook Research Institute, ysyang@sri.utoronto.ca. P. E. Radau, Sunnybrook Research Institute, perry.radau@gmail.com. J. Barry, Sunnybrook Research Institute, jgbarry70@gmail.com. J Detsky, University of Toronto, jsdetsky@gmail.com. G. H. Griffin, University of Toronto and Sunnybrook Research Institute, greg.griffin@sri.utoronto.ca. E. Crystal Sunnybrook Health Sciences Centre, eugene.crystal@sunnybrook.ca. G. A. Wright, Sunnybrook Research Institute, gawright@sri.utoronto.ca.

II. Methodology

In this study myocardial infarction was generated by 90-minute coronary artery occlusion followed by reperfusion in 5 swine (20-25 kg) (in accordance with the animal research protocol guidelines approved by Sunnybrook Health Sciences Centre) [7].

A. Image Acquisition

MRI was performed on a 1.5T scanner (CV/I, GE Healthcare, Mikwaukee, WI) using a surface coil, 4 to 5 weeks after the infarction. Delayed enhancement imaging was started 10 minutes after the injection of 0.2 mmol/kg of Gd-DTPA (Magnevist, Berlex Inc., Wayne, NJ). Between eight to ten short-axis images were acquired to cover the entire left ventricle with the MCLE sequence. MCLE uses steady-state free precession (SSFP) readouts during the inversion recovery process. It produces 20 images over the cardiac cycle, each at a different inversion time. The images at early inversion times have varying contrast where MI can

be visualized as an area of fast T_1 recovery. The following imaging parameters were used: TE=1.9ms, TR=5.5ms, NEX=1, FOV=320mm, 256x256 acquisition matrix, and 5mm slice thickness. The inversion pulse was placed such that the infarct-enhanced images are acquired during diastole, for which TI ranged from 175 to 250 ms.

In this study we used an improved method, MCLE, which has been proven to be superior to conventional DE in characterizing infarct areas [6]. With MCLE, there is no need to acquire test images to optimize TI (Inversion Time) for LE because images at multiple TIs are acquired. With multiple varying TI contrasts this new sequence has been shown to be more sensitive for detecting small subendocardial infarct. In the conventional sequence, semi-automatic algorithms are proposed to quantitatively analyze the total infarct volume [8]. However, these algorithms are both sensitive to image noise. In MCLE, a scatter plot of longitudinal relaxation time (T_1) versus steady-state value for each pixel was used as the input to a fuzzy C-means algorithm to automatically characterize each pixel as infarct, healthy myocardium, and blood. The BZ was defined as pixels that have a significant probability of belonging to both the infarct and healthy myocardium clusters.

B. *In vivo Electro-anatomical Voltage Mapping*

The EP study was then performed (after MCLE imaging) using CARTO EAVM. During sinus rhythm the voltage and activation maps were acquired with catheters inserted endocardially into the left ventricle (LV).

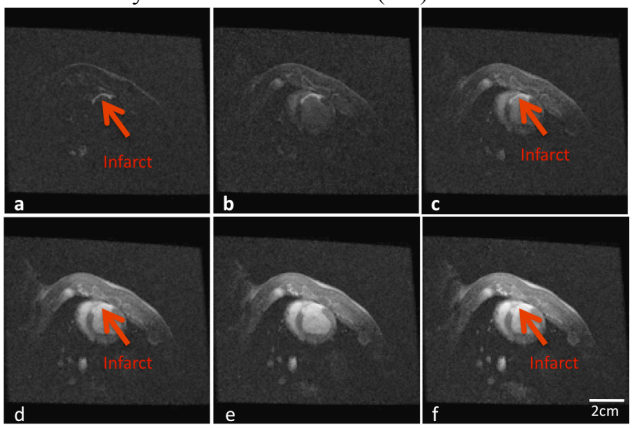

Fig. 1: Six consecutive short-axis MCDE images (a-f) acquired in a porcine model with an anterior infarct. All of the MCLE images are in short-axis view obtained at 1mm x 1mm in-plane resolution with the areas of infarct marked by an arrow. The infarct can be visualized as a hyper-enhanced region in (a-c)). Note the simultaneous nulling of healthy myocardium and blood in image (a)

Cardiac electrograms are generated by the potential (voltage) differences recorded at two recording electrodes during the cardiac cycle in EP studies. During this "electrical mapping", the electrophysiologist instigates the propagation of the action potential wave through recording during sinus rhythm or pacing. LV mapping was performed using a retrograde aortic approach. CARTO, a 3 dimensional mapping system, uses a cathter with a 4- or 3.5 mm tip electrode and 2-mm ring electrodes separated by 1 mm (Navistar or QuickStar, Biosense Webster) in all animal models. Bipolar electrograms recorded by the distal electrode pair of the mapping catheter were filtered to measure only signals within 30-400 Hz. Endocardial regions with bipolar electrogram amplitude greater than 1.5 mV were defined as "normal." The signature of scar in the ventricle is a low-amplitude, high frequency electrogram, with amplitude $\leq$0.5 mV. Low amplitude voltages show some correlation with the degree of slow conduction in and around the area of fibrosis. BZ is defined as a region with bipolar electrogram amplitude between 0.5 and 1.5 mV [9].

C. *Analysis of Infarct heterogeneity in MRI and CARTO*

MCLE produces 20 images over the cardiac cycle, each using a different TI. The images with short TI have varying contrast where MI can be visualized as an area of fast T_1* (which is shorter than the true T_1 due to the continuous SSFP readout) recovery. Between six and eight images were used to extract the signal intensity (SI) recovery for each pixel within the LV, including the blood pool pixels (Fig. 1).

In Figure 2.a scatter plot of T_1* versus steady-state (SS) values for all pixels within the LV is shown, Figure 2.b shows the corresponding spatial map of the various tissue types classified using automated fuzzy clustering analysis.

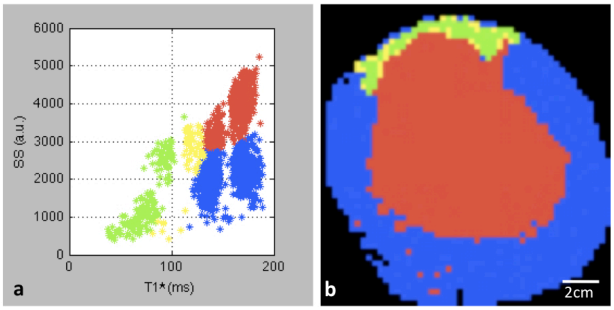

Fig. 2 (a Scatter plot of T_1* versus steady-state (SS) values (data from the same model shown in Fig. 1) for all pixels within the left ventricle, and (b) the corresponding spatial map of the various tissue types classified using automated fuzzy clustering analysis. Infarct (green), healthy myocardium (blue), blood (red), BZ (yellow)

D. *Comparison between CARTO maps and MRI data*

To compare the areas of BZ and infarct in the two methods we calculate the relative extent of each region around the circumference in selected short axis sections. Percentage of circumference on each slice covered by infarct and BZ in each MR slice was calculated by drawing a circle roughly corresponding to the short axis and manually identifying the

angle subtended by infarct and BZ filling at least 50% of the transmural extent of the wall. The ratio of this angle to 360 degrees is the percentage of circumference associated with each region. For CARTO data, we manually draw a contour around the EAVM map and calculate the percentage of scar over the total circumference. This percentage was calculated in the same way for the BZ area.

We correlated the percentage of circumference of BZ and infarct for each slice in MR with the corresponding level (based on the distance from the apex) on the EAVM data set. We depict the correlation plot for the percentage of infarcted region calculated in both MCLE and EAVM. We also plot the relationship of the BZ determined from the MCLE vs. that from EAVM. The correlation coefficient was calculated across all the pigs and their corresponding slices for both the infarct zone and BZ.

E. Histology

The short-axis view slice was prepared for whole-mount histology and was stained with Masson's Trichrome for visualization of collagenous fibers. The samples (cut at 5μm) were scanned at 2-10μm resolution and saved as multi-resolution digital images [10].

III. Results

Here we present results from 5 swine. In MCLE analysis and classification, average T_1* values for each class were obtained in multiple slices. For the particular study with the scatter plot shown in Fig. 2(a), healthy myocardium had an average T_1* value of 144.9±29.9 [ms], scar area had an average T_1* value of 121±27.2 [ms] and BZ average T_1* was 126.1±23.1 [ms].

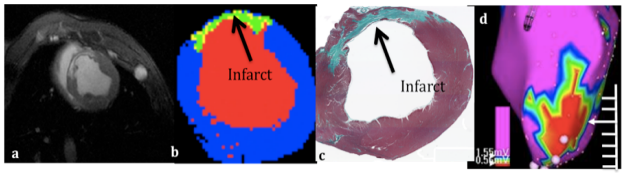

Fig.3: a) Original MCLE image of infarct. b) Classification result with blood in red, infarct in green and BZ in yellow. c) depicts the histology with the green area corresponding the infarct zone. d) illustrates the surface measured voltage map; purple area depicts healthy myocardium and red represents infarct zone.

Fig. 3(a) depicts the classification result with the infarcted region marked in green. The areas of infarct and BZ have good correlation between the MCLE classification result and histology, shown in Fig. 3(b). Green areas in Fig. 3(b) depict areas of infarct. The arrow in Fig. 3(c) shows the area corresponding to the MCLE slice that was imaged.

Fig. 4(a) plots the EAVM BZ vs. the MCLE BZ for all pigs, with different colors corresponding to different pigs. The correlation coefficient for BZ determined by MCLE vs. EAVM was calculated to be 0.7457 with ($p<0.0001$). The line of best fit was drawn on the plot. The slope±SD for this line was 0.83±0.045.

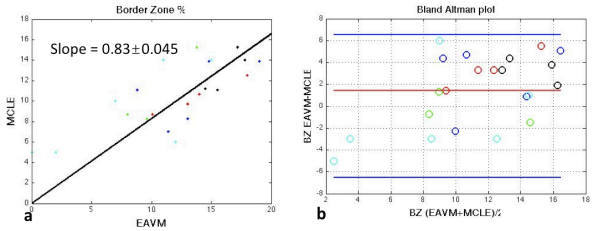

Fig. 4: (a) and (b) show the results for BZ. (a) is the plot of percentage of BZ between EAVM and MCLE with each color point represent a slice within one pig. b represents the Bland Altman for comparing BZ of EAVM and MCLE (mean = 1.45%, SD = 3.26%).

Fig. 5(a) plots the EAVM vs. the MCLE infarct extent for all the pigs. The different colors in the points represent different pigs. The correlation coefficient for the infarct area was 0.7529 ($p < 0.0002$). The line of best fit was drawn on the plot. The slope±SD for this line was 0.77±0.082. This result shows that infarct size measured with two methods was closely related.

A Bland-Altman plot is shown in Fig. 4(b) for comparing the BZ area of EAVM and MCLE. There is a bias between the size of BZ on EAVM compare to the size of BZ on MCLE; suggesting that EAVM might yield slightly bigger percentage BZ that MCLE.

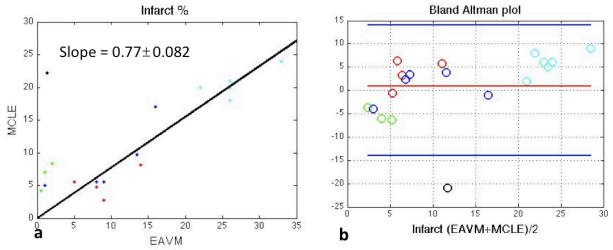

Fig. 5(a) and (b) show results for infarct. a is the plot of percentage of infarct between EAVM and MCLE with each color point representing a slice within one pig. b) represents the Bland-Altman for comparing infarct of EAVM and MCLE (mean = 0.96%, SD = 7.02 %).

Fig. 5(b) shows the Bland-Altman plot comparing the infarct extent as percentage of circumference for EAVM and MCLE. Again, there is no significant bias between he measurements; however there was one outlier. For one of our pig models there was a subtle infarct in which EAVM could not elucidate the infarct area deep in the myocardium due to limited sensitivity and spatial resolution.

Fig. 6(c) illustrates the EAVM of the subtle infarct model. As shown on the map there is not much area marked as infarct (1%); most of the faulty electric sites are characterized as BZ. Fig 6(a) represents the corresponding MCLE slice. MCLE classification depicts an area of narrow infarct deep in the subendocardium while the areas of myocardium close to

endocardium are classified as BZ.

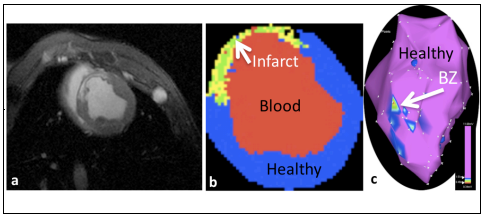

Fig. 6: Illustration of the pig data with a subtle infarct. a) One of the MR images of the pig. A narrow band of scar area can be clearly seen. b) represents the classification result from MCLE. c) On the EAVM we can observe the BZ but not the scar area (for colors please refer to Fig3).

IV. Discussion

On DE-MRI, enhanced infarct can be separated into infarct core and BZ. This is identified with accumulation of contrast agent and signal intensity elevation in the infarct area. The characteristics of the BZ have been shown to correlate with all-cause mortality post-MI [4]. Sinus-rhythm EAVMs were found to identify infarct areas in animal models [11], [12]. For human studies Codreanu et. al [5] were the first to compare the high-density EAM scar definition, using multiple electrogram parameters, against a gold-standard technique based on tissue characterization. They concluded that EAVM compared to conventional DE-MRI provides only a rough delineation of infarct area. In this study, we compare results from EAVM with a new method, MCLE, which has several potential advantages: (1) MCLE yields multiple image contrasts, including the simultaneous nulling of signal from healthy myocardium and blood, which improves the visualization of infarcted tissue compared to conventional DE-MRI; (2) with the fuzzy clustering technique in MCLE, image noise has a smaller impact on BZ analysis; (3) Quantitative T_1* maps may more accurately reflect the relative fraction of fibrosis within a volume.

For a case of subtle infarct, there were either no or only very small areas of infarct identified on EAVM (percentage of infarct in one slice was only 1.3% on EAVM). Meanwhile, MCLE images nicely represent the areas of infarct deeper in the myocardium with some areas of BZ closer to endocardium. The EAVM map having very little infarct (1.3%) had 22.2% of the circumference infarcted on the corresponding slices from MCLE slice. Therefore, percentage of infarct on MCLE doesn't necessarily relate to percentage of infarct on EAVM. It appears that EAVM does not correctly predict the infarct zone when the infarct is less than transmural. This likely has one of two causes: poor resolution since EAVM heavily undersamples the endocardial surface and/or poor sensitivity since the bipolar electrode cannot detect faulty electrical sites deep in the myocardium.

V. Conclusion

MCLE identifies the scar heterogeneity in porcine models and provides additional information to EAVM. In order to permit a quantitative comparison between T_1 maps and EAVM in future studies, more accurate registration must be performed between the two data sets.

Acknowledgment

The authors of this paper would like to acknowledge grant support from the Canadian Institutes of Health Research and the Ontario Research Fund as well as useful discussions with Garry Liu.

References

[1] Bolick DR, Hackel DB, Reimer KA, Ideker RE. Quantitative analysis of myocardial infarct structure in patients with ventricular tachycardia. Cir- culation. 1986;74:1266–1279.

[2] Stevenson WG Ventricular scars and ventricular tachycardia Transaction of American Clinical Association. 2009, 120, 403-12.

[3] de Bakker JM, van Capelle FJ, Janse MJ, Wilde AA, Coronel R, Becker AE, Dingemans KP, van Hemel NM, Hauer RN. Reentry as a cause of ventricular tachycardia in patients with chronic ischemic heart disease: electrophysiologic and anatomic correlation. Circulation. 1988;77:589-606.

[4] Yan AT, Shayne AJ, Brown KA, Gupta SN, Chan CW, Luu TM, Di Carli MF, Reynolds HG, Stevenson WG, Kwong RY. Characterization of the peri-infarct zone by contrast-enhanced cardiac magnetic resonance imaging is a powerful predictor of post-myocardial infarction mortality. Circulation. 2006;114:32-9.

[5] Codreanu A, Odille F, Aliot E, et al. Electroanatomic characterization of post-infarct scars comparison with 3-dimensional myocardial scar reconstruction based on magnetic resonance imaging. J Am Coll Cardiol 2008;52:839–42.

[6] Detsky JS, Stainsby JA, Vijayaraghavan R et al., "Inversion-recovery-prepared SSFP for cardiac-phase-resolved delayed-enhancement MRI," Magnetic Resonance in Medicine, 2007; 58 (2), 365-372.

[7] Pop M, Sermesant M, Mansi T, Crystal E, Detsky JS, Yang Y, Fefer P, McVeigh ER, Dick AJ, Ayache N, Wright GA Characterization of porcine infarcts heart: insights from experiments and theoretical modelling in Proceedings of the FIMH, June 3-5 2009, Nice - LNCS 2009 vol 5528: 1-10.

[8] Kim RJ, Fieno DS, Parrish TB, Harris K, Chen EL, Simonetti O, Bundy J, Finn JP, Klocke FJ, Judd RM. Relationship of MRI delayed contrast enhancement to irreversible injury, infarct age, and contractile function. Circulation. 1999;100:1992-2002.

[9] Verma, A. and Kilicaslan, F. and Schweikert, R.A. and Tomassoni, G. and Rossillo, Short-and long-term success of substrate-based mapping and ablation of ventricular tachycardia in arrhythmogenic right ventricular dysplasia, Circulation. 2005; 111: 24-3209.

[10] Clarke GM, Chris P, Mawdsley G, E. et al., Design and characterization of a digital image acquisition system for whole-specimen breast histopathology Physics in Medicine and Biology, 2006 (20), 5089

[11] Callans JD, Ren J-F, Michele J, Marchlinski F, Dillon S. Electroana-tomic left ventricular mapping in the porcine model of healed anterior myocardial infarction. Correlation with intracardiac echocardiography and pathological analysis. Circulation 1999;100:1744–50.

[12] Wrobleski D, Houghtaling C, Josephson ME, Ruskin J, Reddy V. Use of electrogram characteristics during sinus rhythm to delineate the endocardial scar in a porcine model of healed myocardial infarction. J Cardiovasc Electrophysiol 2003;14:524–9.